International Journal of Physical Research, 2 (2) (2014) 56-66
©Science Publishing Corporation
www.sciencepubco.com/index.php/IJPR
doi: 10.14419/ijpr.v2i2.3079
Research Paper

Synthesis and characterization of CdS-PABS/MWCNT for solar cell applications

K. Babu *, S. Pradeep, S. Bhuvaneswari

Department of Physics, K.S.Rangasamy College of Arts & Science (Autonomous), Tiruchengode-637215, Tamilnadu, India
**Corresponding author E-mail: babuphysics007@gmail.com*

Abstract

Cadmium sulfide (CdS)-Poly (amino benzene sulfonic acid) (PABS) was successfully synthesized and wrapped with functionalized Multi-walled carbon nanotubes (MWCNTs) to form water-soluble composites. Nanocrystalline Cadmium sulfide (CdS) powder has been synthesized by a sol-gel process in which cadmium acetate and has been used as a parent sources for Cd^{2+} and thiourea has been used as a source of S^{2-} . The synthesis of poly (m-amino benzene sulfonic acid) (PABS) by aniline initiated polymerization of m-amino benzene sulfonic acid using ammonium persulfate oxidation has been attempted for the different concentration of aniline (15-20mol% of ABS). The structural analysis of the CdS, water soluble PABS and MWCNT/CdS-PABS have been investigated using spectroscopic techniques and structural techniques such as, UV-Vis spectroscopy, FT-IR spectroscopy, X-ray diffraction (XRD), Photoluminescence (PL) and Thermal analysis (TG-DTA). The CdS-PABS/MWCNT composites synthesized by the present investigations are highly expected to contribute towards the improvement in the solar cell applications.

Keywords: *CDS, ABS, MWCNT, Sol-Gel Process, Ammonium Per sulfate.*

1. Introduction

Due to transparency in the visible and high infrared reflectivity, acoustic characteristics, high electrochemical stability and excellently electronic properties, CdS has been attracted for research and application. It has been widely used in chemical sensor [1], surface acoustic wave device [2] and photoanode films of solar cell [3], [4]. Different techniques are to including sputtering [5], chemical vapor deposition (CVD) [6] and spray pyrolysis [7], [8]. However, among these techniques, the sol-gel process is particularly attractive due to different reasons; good homogeneity, ease of composition control, low processing temperature, large area coatings, low cost efficient in producing thin, transparent, multi-component oxide layers of many compositions on various substrates. CdS nanostructures are regularly n-type due to sulfur vacancies. The variation of the Cd/S concentrations will presumably modify the physical properties of CdS nanostructures, such as morphology, analysis and optical properties. These concentrations will also have an effect on the structural and optical properties of the CdS nanostructures.

Conducting polymers are of interest in fields such as energy storage, sensor, electronic devices, electronic magnetic interference shielding and the inhibition of corrosion. Among the conducting polymers Polyaniline has drawn special attention due to its high stability toward air and moisture, high electrical conductivity and unique redox properties [9].

Polyaniline has emerged in recent years as one of the more promising conducting polymers due to its environmental stability and respectable levels of conductivity, but the solubility of the conducting polymers is of crucial importance for their applications.

These polymers have poor solubility in common organic solvents. Conducting polymers which are soluble in water are more important and versatile, with regards to applications, than those soluble in organic solvents [10]. Several substituted PANIs soluble in organic solvents have been prepared such as alkyl [11], alkoxy [12-15] and alkyl-N-Substituted [16] PANIs.

The most important work in this direction is the synthesis of the sulfonated PANIs (SPAN) [17-21].SPANs are of interest because of their unique electroactive properties, Self-doping, thermal stability, characteristic optical properties

and water solubility. SPANs have potential applications in rechargeable batteries [22], [23], light emitting diodes [24], junction devices [25]. However, because the sulfonic acid functionality is a strong electron-with drawing group, the conductivity of SPAN (10-3 to 10-7 Scm-1) is much lower than that of PANI (10-1 to 10 Scm-1). Carbon nanotubes (CNTs) take a variety of forms single wall (SWCNTs), double wall (DWCNTs) and multi-wall (MWCNTs).where the cylindrical concentric planes interact with each other due to the van der Waals forces. Nanotubes and their modified structures are characterized by the following properties: real density similar to that of a polymer, electrical conductivity better than that of copper, excellent flexibility and elasticity, excellent chemical stability, both of metal and semiconductor, a high aspect ratio (50–1000), mechanical strength better than that of steel, excellent thermal conductivity, excellent electron emission [26], [27]. These parameters make carbon nanotubes a very attractive material for numerous applications. CNTs are starting to be used in nanotechnology, nanoelectronics, nano optoelectronics, nano biotechnology, catalysis and as a sorbent Potential practical applications of CNTs include their use as chemical sensors, field emission materials, catalyst supports, electronic devices, high-sensitivity nanobalances for nanoscopic particles, nanotweezers, reinforcements in high-performance composites and as nanoprobes in metrology and biomedical and chemical investigations, In this paper, we report the water soluble conducting polymer, poly (m-amino benzene sulfonic acid) (PABS) and it is highly expected for ammonia sensor.

2. Experimental section

Materials Used

Cadmimum acetate (Cd (CH3 COO) 2.2H2O) and thiourea (CH4N2S) from spectrum reagents and chemicals pvt.ltd, Aniline, Acetone Nice laboratories Pvt. Limited, methanol from cheme pure laboratories was used as received. Amino benzene sulfonic acid (ABS) from Lobo, Hydrochloric Acid (HCl) from nice chemicals, Ammonium Persulfate (APS) from spectrum, Multiwalled carbon nanotube (MWCNT) from sisco research laboratories pvt.ltd Mumbai was used as received. All the chemicals were used for this experiment without any further purification. All the chemicals were used for this experiment without any further purification.

2.1. Synthesis of CdS nanoparticles

2.1.1. Procedure

Nanocrystalline CdS powder has been synthesized by a sol-gel process in which cadmium acetate (Cd (CH3 COO) 2.2H2O) has been used as a parent source for CdS and thiourea (CH4N2S) has been used a source of s. For experiment, 3.198 gm of cadmium acetate and 1.824 gm of thiourea was added into 40 ml of methanol and mixture was stirred vigorously at 60°C for 1h (gel formation). After gel formation heating was stopped and the solution was stirred continued until we get a yellow powder. The powder was dried in zone furnace at 400°C for 30 min to get the nano crystalline CdS powder having particles of size of 40-50 nm.

2.2. Synthesis of PABS

In our present study, PABS was synthesized from the monomer m-Amino benzene sulfonic acid. ABS normally does not polymerize possibly due to the bulky and electron withdrawing SO-H substituent, which hinders the oxidation. But in the presence of a few drops of aniline (15–20) mol% of ABS it is polymerized in 1 M HCl using ammonium persulfate as an oxidant, with excellent yield as initiator for oxidative polymerization of a monomer with higher oxidation potential explored (70–75%).

For the synthesis of PABS, m-Amino benzene sulfonic acid (0.865gram) and aniline (15-20 mol % of ABS) were mixed in 1M HCl with ammonium persulfate as the oxidation reagent. Aniline was used as the initiator for the ABS polymerization. The mixture was stirred at 0°C for 6 hours and then the solution was concentrated at room temperature, filtered, and the solid was washed with acetone. The obtained polymer itself is highly water soluble, giving a pink solution as shown in the flowchart. The solid that collected on the filter paper was redissolved in water and then reprecipitated by slow addition of the aqueous solution to a large excess of acetone. The black precipitate was collected by filtration and dried at room temperature.

During the synthesis of PABS color changes were absorbed when adding the ammonium persulfate (oxidation reagent) into the mixture of ABS and Aniline. On adding 1ml of APS the color of the solution changed into pink and after that for the addition of 6.2 ml of APS it changed into light violet color. For the further addition of APS for an amount of 7.2ml, 11ml, 13ml, 17.2ml the color was changed to violet, blue, blue with black and black respectively as shown in figure 1. This color changes resembles the formation of polymer.

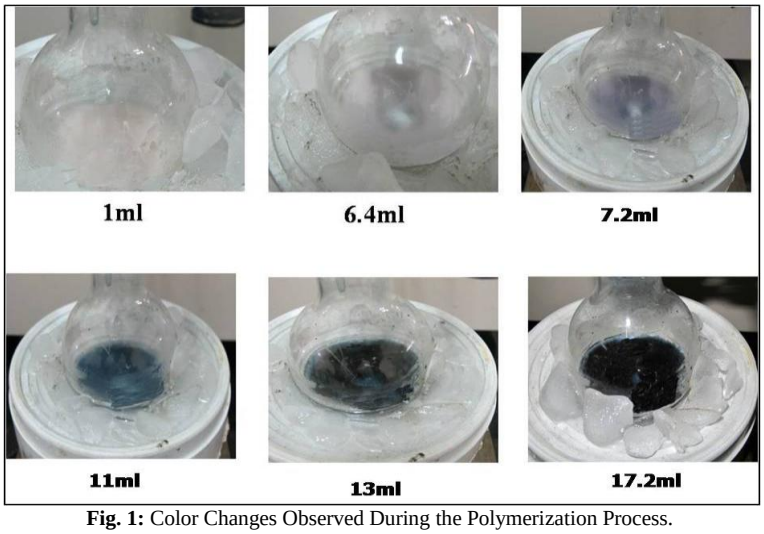

Fig. 1: Color Changes Observed During the Polymerization Process.

2.2.1. Solubility test

The polymers are soluble in H2O, DMF and 0.1 N of NaOH. Base form of this polymer gives a deep violet colour in solution. The solubility of the polymer on these solvents is clearly shown in figure 2.

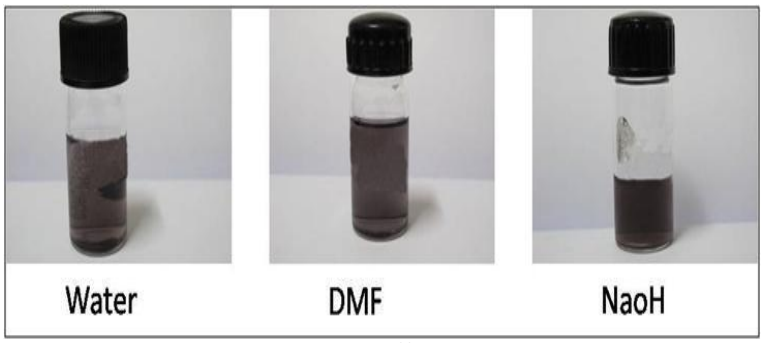

Fig. 2: PABS in Different Solvents.

2.3. Synthesis of CdS/PABS

2.3.1. Procedure

Different amount of CdSwere dispersed into the APS solution and stirred for 1 hour prior to the addition of aniline. Aniline (0.4mol) stirred with 0.4 mol PABS in 20ml of Distilled water were added drop-wised using burette into the APS-CdS solution and stirred vigorously to form homogeneous dispersion.

During the synthesis of CdS-PABS color changes were absorbed when adding the PABS into the CdS solution. Initially CdS color is yellow when adding 1ml of PABS solution into CdS the color of the solution changed into yellow with black. For the further addition of PABS for an amount of 2ml, 13ml and 20ml for the addition of PABS color was changed to black color. (Figure 3)

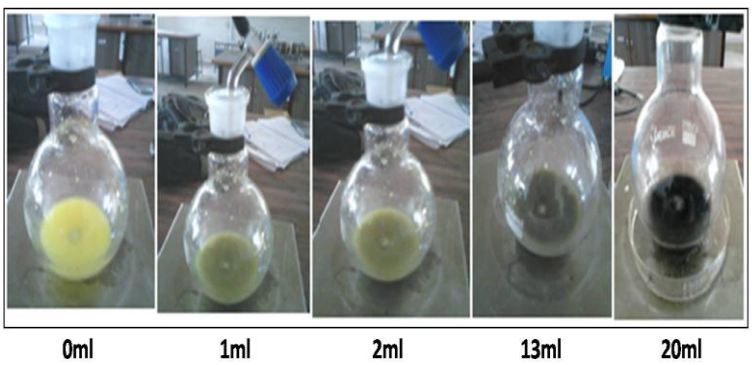

Fig. 3 Color Changes Observed During PABS Added Into CdS

2.4. Synthesis of CdS-PABS/MWCNT

2.4.1. Procedure

The commercially available MWCNT used in this study were of high purity (>95%) and used as it is without further purification supplied sisco research laboratories pvt.ltd Mumbai. The functionalization of MWCNT was accomplished using cetyltrimethylammoniumbromide (CTAB) as a functionalizing agent. Functionalization was performed using 1:10 proportion of MWCNT with CTAB and 1:100 ratios of solute with solvent (methanol).The complete mixture was sonicated for 30 min. After sonication, the functionalized MWCNT were centrifuged and washed with methanol for number of times, all the residue (functionalized MWCNT) was collected.
For the preparation of CdS-PABS/MWCNT nanocomposites using simple chemical route used. For an equimolar amount of CdS-PABS in 20 ml methanol were mixed. After stirring the solution or few min., an appropriate amount of functionalized MWCNT was added into the solution. After mixing for 60 min at constant temperature (70˚ C) with continuous stirring, the composite were centrifugally separated, washed repeatedly with methanol, and dried in air at room temperature.

3. Result and discussion

3.1. Spectroscopic analysis of CdS

3.1.1. UV-VIS spectroscopy

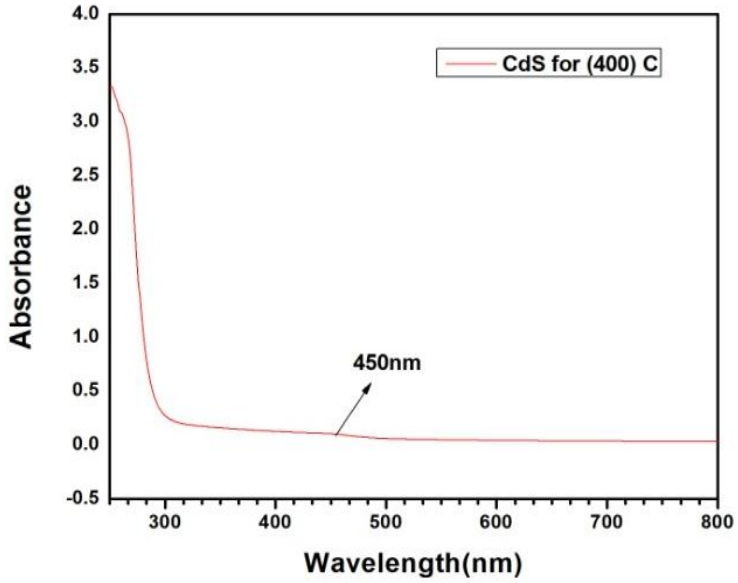

Fig. 4: UV-VIS Spectrum of CdS

As shown in Figure 4, blue shift in the maximum absorption band 450 nm occurs as the concentration of organic ligand increases. The absorption peaks of three samples of different molar ratios of ligand to Cd2+ are centered at 450 nm, respectively. The blue shift is consistent with the quantum confinement effect due to decreasing particle size because the higher concentration of ligand is unfavorable to the nucleation and growth of CdS.

3.1.2. Fourier transform infrared (FTIR) spectroscopy

The Fourier transforms infrared spectroscopy (FTIR) for different prepared materials are discussed here. Figure 5 shows the FTIR spectrum in the frequency range (400–4000 cm-1) of Nanocrystalline CdS synthesized by Spectrum RXI model. There is a band at 615.53 cm-1 is due to the stretching frequency of Cd-S bond. Strong interaction of water with CdS is reflected by peaks at 3428.11 cm-1 and 1628.28 cm-1 due to O–H stretching and O–H bending modes, respectively. In the higher energy region the peak at 3428.11 cm-1 is assigned to O-H stretching of absorbed water on the surface of CdS. The C-O stretching vibration of absorbed methanol gives its intense peak at 1107.87 cm-1.

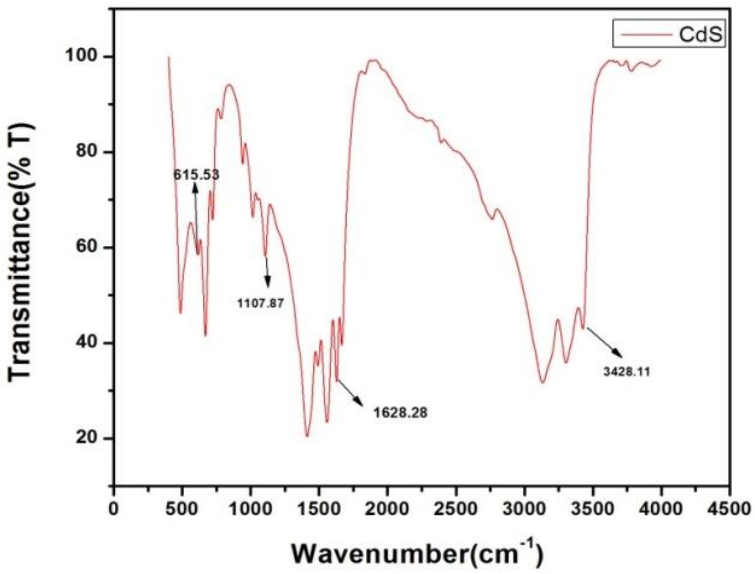

Fig. 5: FT-IR Spectrum of CdS in Different Concentrations

Table 1: Mode Assignment of CdS

Material/Functional Group	CdS cm-1
Cd-S	615.53
O–H stretching	3428.11
O–H bending	1628.28
C-O stretching	1107.87

3.1.3. Structural analysis of CdS

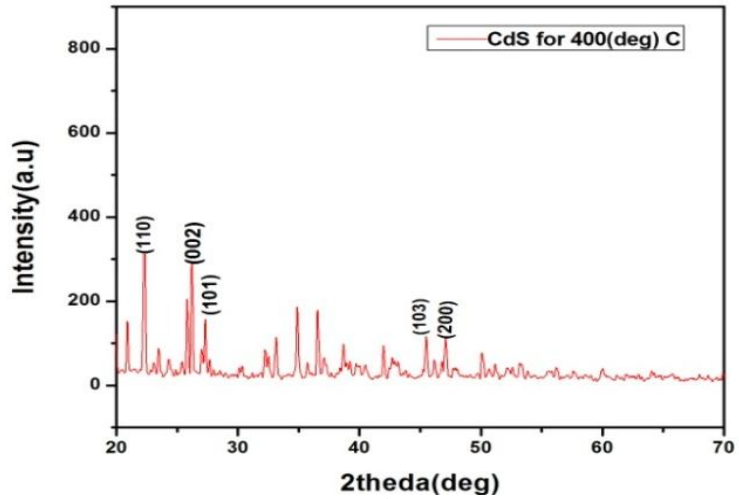

Fig. 6: XRD Spectrum for CdS Nanoparticle.

Figure 6 shows the X-ray diffraction (XRD) patterns for as prepared sample. The data was collected over a 2θ range 20-70˚. The XRD patterns of nano CdS nanocomposites exhibit the characteristic peaks for crystalline CdS of hexagonal wurtzite structure. For the first signal results from (110) CdS at 23.6˚. The remaining two at 26.1̊ (002) and 27.1˚ (101). The presence of such interaction can also be studied by the crystal aspect ratio which is defined as the ratio of crystallite size in the (002) and (101) planes of X-ray diffraction pattern. From the observed XRD peaks (101) and (002), the lattice constants were obtained as a = b = 4.141 Å, c = 6.681 Å for the CdS. The average crystallite size of the CdS nanoparticles was calculated by using well known Debye-Scherrer formula and is found to be 14.22nm.

3.2. Spectroscopic analysis of PABS

In our present work, we have synthesized water soluble conducting polymer CdS- PABS and we have grafted the polymer on MWCNTs in order to improve the conductivity of the composites MWCNT was added. The resultant MWCNT-CdS/PABS composites also water soluble which has found an application for solar cell applications.

The structrual characterization of synthesizedCdS-PABS analysed by both spectroscopic and microscopic techniques. The presence of functional groups were analysed by using UV-VIS and FT-IR spectroscopic techniques. Table 1 shows Different parameters adopted for the synthesis of PABS.

Table 2: Different Parameters Adopted for the Synthesis of PABS

Parameters	A
Aniline concentration	20 mol% of ABS
Initial mixing time (aniline + ABS)	30 minutes
Oxidation time	6 hours
Amount of ABS	0.865g

3.2.1. UV-VIS spectroscopy

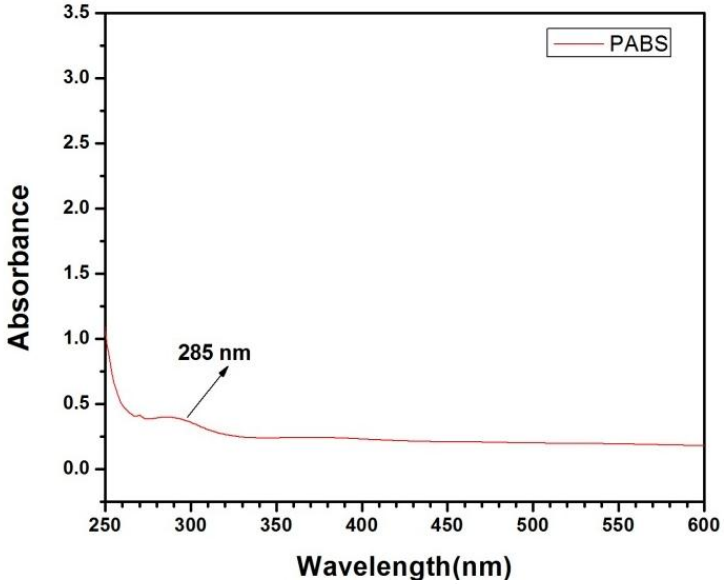

Fig. 7: UV-VIS Spectrum of PABS

From the UV-VIS spectrum it is finalized that, for the aniline concentration of about 20mol% of ABS gives complete formation of PABS so further synthesis was done for this concentration and figure 7 shows the UV-VIS spectrum of neat PABS with its characteristics peaks at 285-297nm in water. In general UV spectrum of PABS consists of two major absorption peaks. One at285–299nm (4.35–4.14 eV) is assigned to the π-π* transition which is related to the extent of conjugation length. The hypos chromic shift of this transition compared to polyaniline is caused by steric hindrance between the large ortho substituent and neighboring phenyl hydrogen, and localization of charge in these structures due to hydrogen bonding interaction between SO3H and NH4+ radical cation by favorable five or six-membered chelate formation, increasing the band gap.

3.2.2. Fourier transform infrared (FTIR) spectroscopy

Infrared spectrum was recorded by using Fourier transform infrared spectrophotometer (model: Spectrum RXI, Make: Perkin Elmer, FT-IR spectrophotometer) to identify the chemical structure of the PABS. The infrared spectrums of the samples were compared with that reported in the literature. The FTIR spectrum for PABS for the concentrations of aniline is shown in figure 8. Strong quinoid bands at 1578.10 cm-1and weak benzenoid absorption at 1520.10 cm-1 are observed in the spectrums. The symmetric stretching vibration of SO2 appears between 1029.33cm-1 and the peaks at 698.98cm-1 and 600.13cm-1are assigned to the characteristic S–O and C–Br stretching modes, respectively. Asymmetric stretching SO21305.53cm-1 may overlap with the characteristic C–N stretching. Only a strong aromatic C–N stretching band appears at 1153.19cm-1.The absorptions at 874.95 and 806.93cm-1 for the C–H out-of-plane bending vibrations corresponding to 1, 2, 4 and 1, 4-sub-stituted benzene rings, indicate that the monomers in the polymers are bonded in head-to-tail fashion, like polyaniline. These results also verify the formation of the conducting polymer PABS.

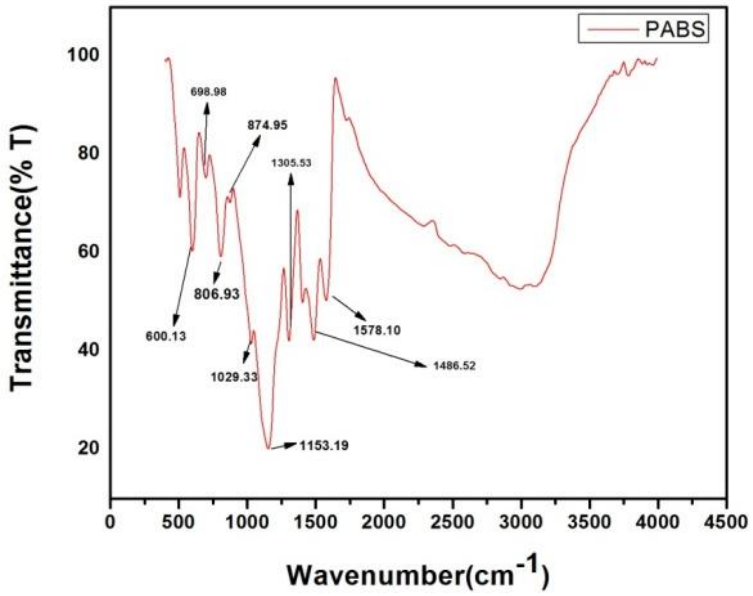

Fig. 8: FT-IR Spectrum of PABS in Different Concentrations

Table 2: Mode Assignments of PABS

Material/ Functional Group	PABS cm-1
Strong Quinoid band	1578
Weak Quinoid band	1486
Symmetric stretching vibration of So2	1029
S-O Stretching	698
C-Br stretching	600
Asymmetric stretching vibration of So2	1305
Aromatic C-N Stretching	1153
C-H Bending vibration (1,2,4) subsitituted rings	874
C-H Bending vibration (1,4) subsitituted rings	806

3.3. Spectroscopic analysis of CdS-PABS/MWCNT

3.3.1. UV-VIS Spectroscopy

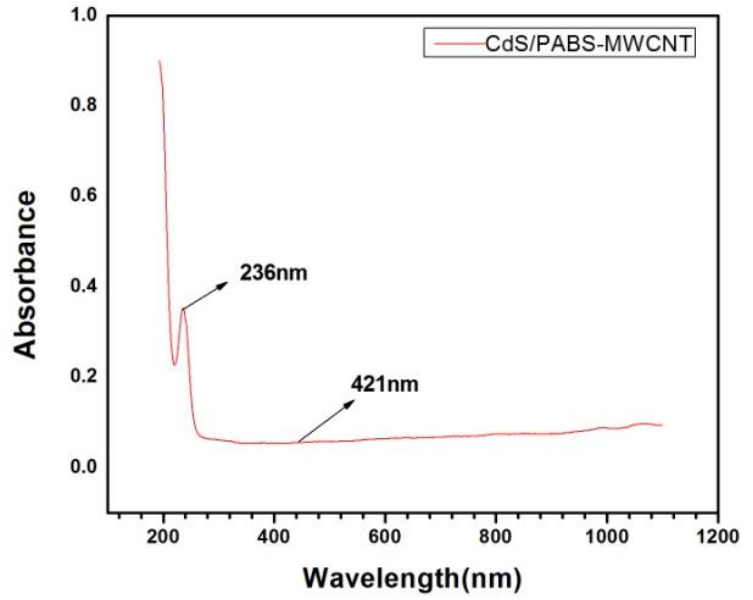

Fig. 9: UV-VIS Spectrum of CdS-PABS/MWCNT

It can be seen from the figure 9 MWCNTs shows characteristic absorption spectrum in 200-800 nm which confirms the in fluence of the CTAB on carbonnanotubes. These spectra monitor the valence to conduction electronic transitions. The continuous increase in absorption in the 236 nm is due to the overlap between the electrons of several double

bonds, which is responsible for π-Plasmon and the weak peak 421nm shows that the optical transition of the CdS particles.

3.3.2. Fourier transform infrared (FTIR) spectroscopy

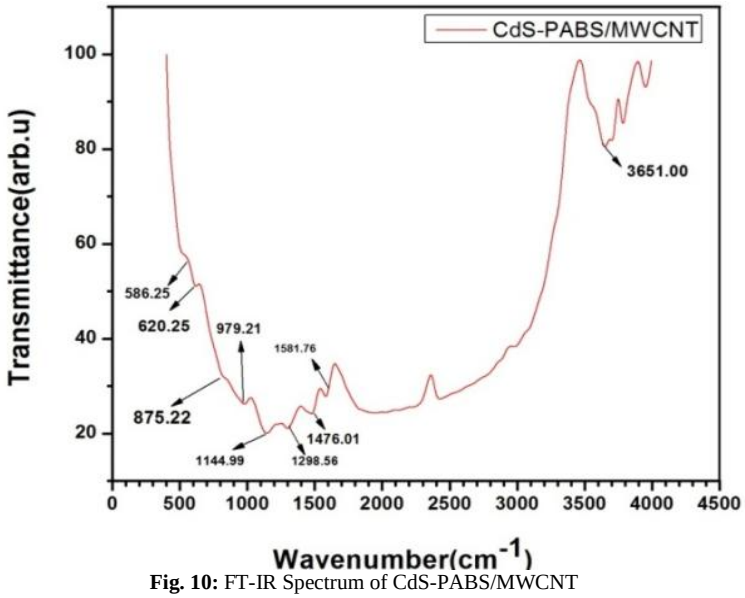

Fig. 10: FT-IR Spectrum of CdS-PABS/MWCNT

The Fourier transforms infrared spectroscopy (FTIR) for different prepared materials are discussed here. Figure 10 shows the FTIR spectrum in the frequency range (400–4000 cm-1) of Nanocrystalline CdS synthesized by Spectrum RXI model. There is a band at 620.25 cm-1 is due to the stretching frequency of Cd-S bond. Strong interaction of water with Cd Sis reflected by peaks at 3651.00 cm-1 and 1581.76 cm-1 due to O–H stretching and O–H bending modes, respectively. In the higher energy region the peak at 3651.00 cm-1 is assigned to O-H stretching of absorbed water on the surface of CdS. The C-O stretching vibration of absorbed methanol gives its intense peak at 1144.99 cm-1.MWNTs show peaks between 979.21, which are described to the phenyl-carbonyl C–C stretching vibrations. Peak observed 1581.56 cm-11476.01 cm-1is due to the carbonic C–C stretching and O–H bending deformation in carboxylic acid groups respectively. The O-H stretching vibration appears at 3651.00 cm-1 as a broad band. In addition, it is clear that the acid treatment on pristine MWNT resulted in the formation of oxygen-containing functional groups at the external walls and at the end caps in the MWNT. Strong quinoid bands at 1581.76 cm-1 are observed in the spectrums. The symmetric stretching vibration ofSO2 appears between1144.99cm-1and the peaks at 620.25cm-1and 586.25cm-1 are assigned to the characteristic S–O and C–Br stretching modes, respectively. Asymmetric stretching SO2 1298.56 cm-1 may overlap with the characteristic C–N stretching. Only a strong aromatic C–N stretching band appears at 1298.56cm-1. The absorptions at 780.18 and 808.26 cm-1 for the C–H out-of-plane bending vibrations corresponding to 1, 2, 4 and 1, 4-sub-stituted benzene rings, indicate that the monomers in the polymers are bonded in head-to-tail fashion, like polyaniline. These results also verify the formation of the conducting polymer CdS-PABS/MWCNT.

Table 3: Mode Assignments of CdS-PABS/MWCNT

Material/ Functional Group	CdS-PABS/MWCNT cm-1
Cd-S	620
O–H stretching	3651
O–H bending	1581
C-O stretching, Symmetric stretching vibration of So2	1144
Phenyl carbonyl C-C Stretching	979
Strong Quinoid band	1581
S-O Stretching	620
C-Br stretching	586
Asymmetric stretching vibration of So2, Aromatic C-N Stretching	1298
C-H Bending vibration (1,2,4) subsitituted rings	780
C-H Bending vibration (1,4) subsitituted rings	808

3.3.3. Structural analysis

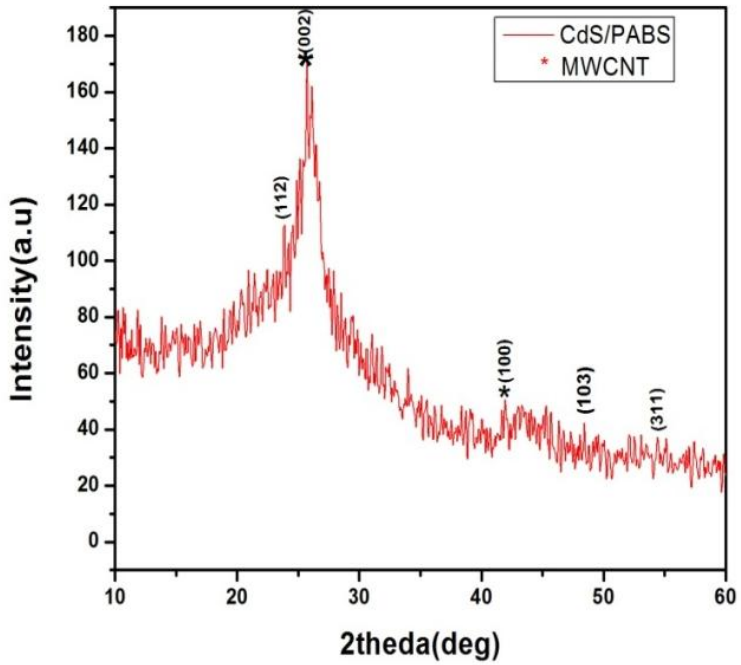

Fig. 11: XRD Analysis of CdS-PABS-MWCNT

Figure 11 shows the X-ray diffraction (XRD) patterns for as prepared sample. The data was collected over a 2θ range 10-60̊.The sample is composed of CdS-PABS nanoparticles on MWCNT's. The XRD pattern demonstrates highly intense peak at 26̊ corresponding to (002) plane and dimensioned peak at 42.9˚ corresponding to (100) plane, which are form MWCNT's. Well defined peaks form XRD in figure shows the nanocrystalline nature for the CdS-PABS particles deposited on MWCNT's. The first signal results from (112) plane of CdS-PABS at 23.6˚, the remaining peak at 48.9˚and 54.2˚ C are indexed to (103) and (311) planes, respectively, are diffused and broadened as the results of the small size of the crystallites. The average crystallite size of the CdS-PABS/MWCNT nanoparticles was calculated by using well known Debye-Scherrer formula ($D=0.94\lambda/\beta\cos\theta$) and is found to be 70μm.

3.3.4. Photoluminescence spectroscopy

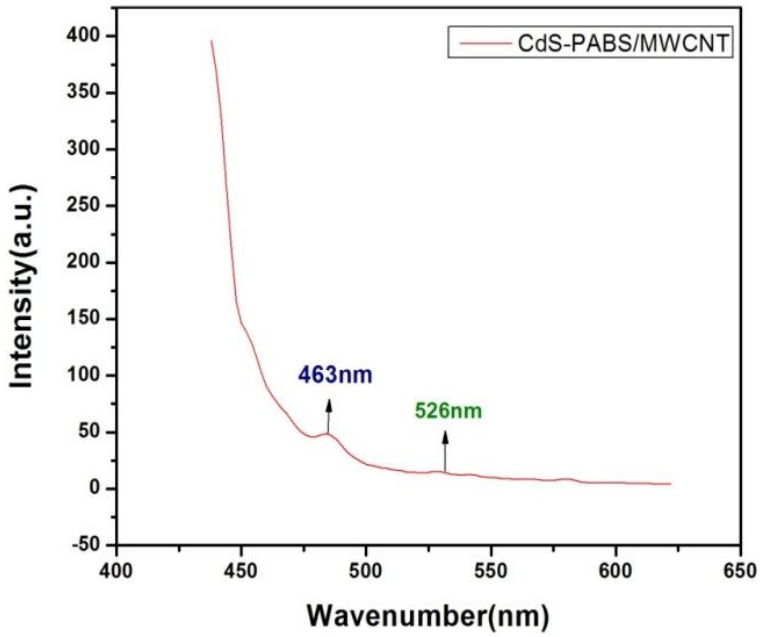

Fig. 12: Photoluminescence (PL) Spectrum of the MWCNT's Nanocomposites upon Light Excitation at 425 Nm

Figure 12 illustrates the PL spectra of CdS-PABS nanoparticles attached to MWCNT's. The PL spectra displays two emission bands including a broad band with a maximum at 463 nm and a shoulder at 526 nm, which could arise from inhomogeneous size of the CdS-PABS nanoparticles on the MWCNT's. The CdS-PABS/MWCNT's nanocomposites exhibit luminescence with a strong emission at 463nm represents for Blue light and a weak emission at 526nm

corresponds to Green light these values can be assigned to trap emission and electron-hole recombination, respectively. In another way, strong emission can be assigned for smaller nanoparticles of CdS-PABS with energy gap of 2.67eV resulting in blue shift as compared to bulk band gap of CdS (2.4eV) due to quantum confinement, Whereas weak emission is assigned towards agglomeration of small nanoparticles to form bigger once resulting in bulk band gap energy of CdS(2.35eV).

3.3.5. TG-DTA analysis for CdS-PABS/MWCNT

The results of TGA analysis for CdS-PABS/MWCNT nanocomposites are shown in Figure 12. In the TGA thermograph of CdS-PABS/MWCNT, it can be observed that the losses of weight occurred around two temperature periods, ranging from 100 to 200°C and around 650 to 750°C. The first weight loss was mainly contributed by the elimination of impurities, residual water and unreacted monomers. MWCNT's are very stable and no decomposition takes place in the range of 200 to 600°C. The second step weight loss which is attributed to the degradation of polymer main chain. The 50% weight loss of Pani is attributed at temperature 3200°C and in case of CdS-PABS\MWCNT nanocomposites it is at 6000°C.This clearly indicated that the thermal stability for the nanocomposites has been improved significantly as higher decomposition temperature in the TGA profile. It might be related to the combination of CdS nanocrystalline in the polymer matrix, which yielded stronger binding force due to the interaction between CdS nanoparticles and the lone pair electrons of N atom in the polymer backbone. For DTA analysis of the CdS-PABS\MWCNT nanocomposites shows the melting point at 461°C which conforms that the presence of PABS.

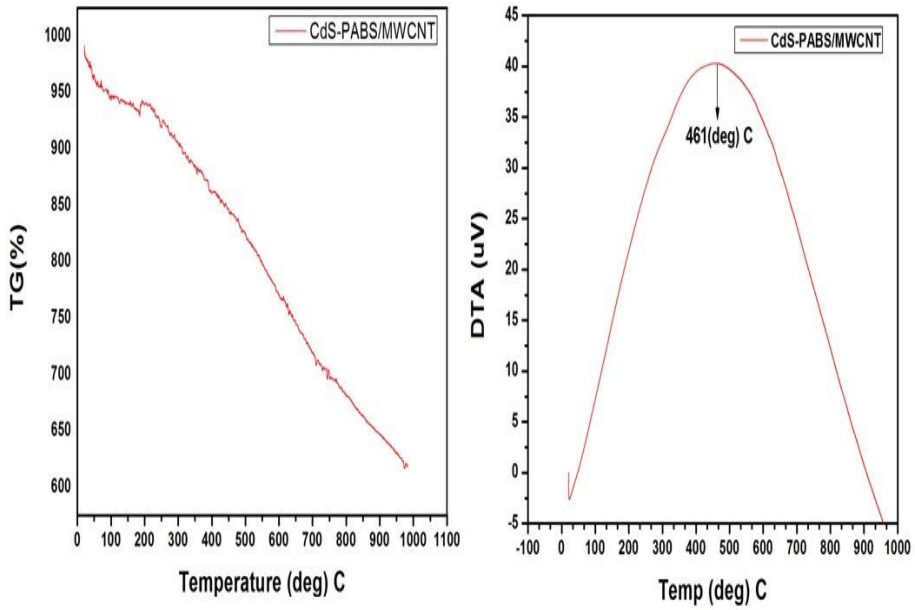

Fig. 13: TG-DTA of CdS-PABS/MWCNT

4. Conclusion

We report the synthesis of cadmium sulfide (CdS) – Poly (amino benzene sulfonic acid) (PABS) composites grafted with f-Multi-walled carbon nanotubes (MWNTs) using CTAB to form water-soluble composites. Nanocrystalline Cadmium sulfide (CdS) powder has been synthesized by a sol-gel process in which cadmium acetate and has been used as a parent sources for Cd 2+ and thiourea has been used as a source of S2- . The synthesis of poly (m-amino benzene sulfonic acid) (PABS) by aniline initiated polymerization of m-amino benzene sulfonic acid using ammonium persulfate oxidation has been attempted for the different concentration of aniline (15-20 mol% of ABS). On the basis of UV-Vis spectroscopic results we conclude that for the aniline concentration of 20mol% of ABS, PABS is completely formed from its monomer. Water soluble PABS and CdS-PABS/MWCNT were thoroughly studied using spectroscopic techniques and structural techniques such as UV-Vis spectroscopy, FT-IR spectroscopy, X-ray Diffraction (XRD), photoluminescence (PL) and thermal analysis (TG-DTA). From the studies it was confirmed that, the CdS-PABS has completely wrapped around the f-MWCNT. The CdS-PABS/MWCNT composites synthesized by the present investigations can be used for the application of solar cells.

References

[1] A. Apolinar-Iribe, M. C. Acosta-Enriquez, M. A. Quevedo-Lopez, R. Ramirez-Bon, A. De Leon, S. J. Castillo, Chalcogenide Letters, 8 (2011) 77.

[2] B. Wacogne, M. P. Roe, A. T. Pattinson, *Applied Physics Letters*, 67 (1995) 1674. http://dx.doi.org/10.1063/1.115053.
[3] L. Stolt, J. Hedstrom, J. Kessler, *Applied Physics Letters*, 62 (1993) 597. http://dx.doi.org/10.1063/1.108867.
[4] K. Keis, Eva Magnusson, H. Lindstrom, S-E. Lindquist, A. Hagfeldt, *Solar Energy Materials and Solar Cells*, 73 (2002) 51. http://dx.doi.org/10.1016/S0927-0248 (01)00110-6.
[5] N. K. Zayer, R. Greerf, K. Rogers, A. J. C. Grellier, C. N. Pannell, *Thin Solid Films*, 352 (1999) 179. http://dx.doi.org/10.1016/S0040-6090 (99)00329-6.
[6] B. M. Ataev, A. M. Bagamadova, A. M. Djabrailov, *Thin Solid Films*, 260 (1995) 19. http://dx.doi.org/10.1016/0040-6090 (94)09485-3.
[7] B. Joseph, K. G. Gopchandran, P. V. Thomas, Peter Koshy, V. K. Vaidyan, *Materials Chemistry and Physics*, 58 (1999) 71. http://dx.doi.org/10.1016/S0254-0584 (98)00257-0.
[8] M. D. Knudson, Y. M. Gupta, A. B. Kunz, *Physical Review* B, 59 (1999) 11704. http://dx.doi.org/10.1103/PhysRevB.59.11704.
[9] G.B.Blanchet, C.R.Fincher, F.Gao,*Appl.Phys.Lett* 2003, 82, 1290. http://dx.doi.org/10.1063/1.1553991.
[10] J. Yue, A. J. Epstein, *J .Am. Chem.Soc*.112.1990. 2800.
[11] Y. Wei, W.W. Focke, G.E. Wnek, *J.Phys.Chem* 189 J.Phys.Chem 1989, 93,495. http://dx.doi.org/10.1021/j100338a095.
[12] S.K. Dhawan, D.C. Trivedi, Synth.Met.1993, 60, 67. http://dx.doi.org/10.1016/0379-6779 (93)91186-6.
[13] W. Feng, A.Fujii, S. Lee,H.C. Wu,K. Yeshino, Synth.Met.2001, 121, 1595. http://dx.doi.org/10.1016/S0379-6779 (00)01502-2.
[14] J.D. Macinnes, B.L.Funt, Synth.Met.1988, 25, 235. http://dx.doi.org/10.1016/0379-6779 (88)90248-2.
[15] G.D. Storrier,S.B. Colbran,D.B. Hibbert, Synth.Met.1994, 62,179. http://dx.doi.org/10.1016/0379-6779 (94)90309-3.
[16] S. Chen,G. Huang,*J.Am.Chem.Soc*.1995, 117, 10055. http://dx.doi.org/10.1021/ja00145a017.
[17] X. Wei,Y.Z. Wang,S.M. Long,C. Bobeczko, A.J. Epstein, *J.Am. Chem. Soc*. 1996, 118, 2545. http://dx.doi.org/10.1021/ja952277i.
[18] S.Ito,K. Murata,S. Teshima,R. Aizawa,Y. Asako, K. Takahashi,B.M. Hoffman, Synth.Met.1998, 96, 161. http://dx.doi.org/10.1016/S0379-6779 (98)00074-5.
[19] Y. Cao,A. Andreatta, A.J. Heeger,P. Smith, Polymer, 1989, 30, 2305. http://dx.doi.org/10.1016/0032-3861 (89)90266-8.
[20] B.C. Roy, M. Dutta Gupta, L. Bhowmik, J.K. Ray, Synth.Met.1999, 100, 233. http://dx.doi.org/10.1016/S0379-6779 (98)01505-7.
[21] B.C. Roy, M.D. Gupta, L. Bhowmik,J.K. Ray, Synth.Met.2002, 130, 27. http://dx.doi.org/10.1016/S0379-6779 (02)00108-X.
[22] C. Barbero,M.C. Miras,R. Kotz,O. Haas, Synth.Met. 1993, 55, 1539. http://dx.doi.org/10.1016/0379-6779 (93)90281-Z.
[23] C. Barbero, M.C. Miras,B. Schnyder,R. Kotz, O.Haas, *J.Mater, Chem*, 1994, 4, 1775.
[24] M. Ferrcira,M.F. Rubner, *Macromolecules*, 1995, 28, 7107. http://dx.doi.org/10.1021/ma00125a012.
[25] M. Narasimhan,M. Hagler,V. Cammarata, M. Thakur, *Appl. Phys.Lett*, 1998, 72, 1063. http://dx.doi.org/10.1063/1.120965.
[26] R.H. Baughman, A.A. Zakhidov, W.A. de Heer, Science 297, 787 (2002). http://dx.doi.org/10.1126/science.1060928.
[27] www.carbonnanotube.biz.